

Rotationally adiabatic pair interactions of para- and ortho-hydrogen with the halogen molecules F₂, Cl₂, and Br₂

Matthias Berg, Antonio Accardi, Beate Paulus, and Burkhard Schmidt

Citation: *The Journal of Chemical Physics* **141**, 074303 (2014); doi: 10.1063/1.4892599

View online: <http://dx.doi.org/10.1063/1.4892599>

View Table of Contents: <http://scitation.aip.org/content/aip/journal/jcp/141/7?ver=pdfcov>

Published by the [AIP Publishing](#)

Articles you may be interested in

Modeling the hydration of mono-atomic anions from the gas phase to the bulk phase: The case of the halide ions F, Cl, and Br

J. Chem. Phys. **136**, 044509 (2012); 10.1063/1.3678294

Communication: Probing the entrance channels of the X + CH₄ → HX + CH₃ (X = F, Cl, Br, I) reactions via photodetachment of X-CH₄

J. Chem. Phys. **134**, 191102 (2011); 10.1063/1.3591179

Chemical Properties of Electronically Excited Halogen Atoms X (2 P 1/2) (X = F, Cl, Br, I)

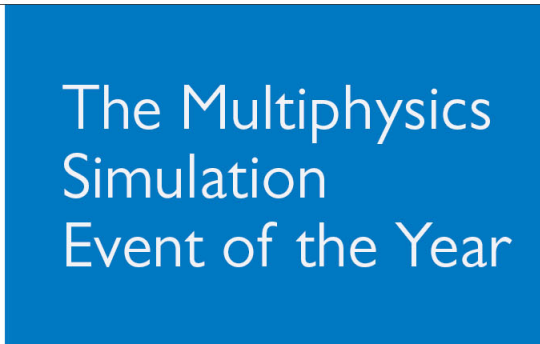
J. Phys. Chem. Ref. Data **35**, 869 (2006); 10.1063/1.2137724

On the structure and physical origin of the interaction in H₂ Cl and H₂ Br van der Waals anion complexes

J. Chem. Phys. **121**, 5852 (2004); 10.1063/1.1784413

TDMP2 calculation of dynamic multipole polarizabilities and dispersion coefficients for the halogen anions F⁻, Cl⁻, Br⁻ and I⁻

J. Chem. Phys. **108**, 3863 (1998); 10.1063/1.475789



COMSOL
CONFERENCE
2014 BOSTON

The Multiphysics
Simulation
Event of the Year

LEARN MORE >>

COMSOL

Rotationally adiabatic pair interactions of para- and ortho-hydrogen with the halogen molecules F₂, Cl₂, and Br₂

Matthias Berg,^{1,a)} Antonio Accardi,^{1,b)} Beate Paulus,^{1,c)} and Burkhard Schmidt^{2,d)}

¹Institut für Chemie, Freie Universität Berlin, Takustr. 3, D-14195 Berlin, Germany

²Institut für Mathematik, Freie Universität Berlin, Arnimallee 6, D-14195 Berlin, Germany

(Received 3 June 2014; accepted 29 July 2014; published online 15 August 2014)

The present work is concerned with the weak interactions between hydrogen and halogen molecules, i.e., the interactions of pairs H₂-X₂ with X = F, Cl, Br, which are dominated by dispersion and quadrupole-quadrupole forces. The global minimum of the four-dimensional (4D) coupled cluster with singles and doubles and perturbative triples (CCSD(T)) pair potentials is always a T shaped structure where H₂ acts as the hat of the T, with well depths (D_e) of 1.3, 2.4, and 3.1 kJ/mol for F₂, Cl₂, and Br₂, respectively. MP2/AVQZ results, in reasonable agreement with CCSD(T) results extrapolated to the basis set limit, are used for detailed scans of the potentials. Due to the large difference in the rotational constants of the monomers, in the adiabatic approximation, one can solve the rotational Schrödinger equation for H₂ in the potential of the X₂ molecule. This yields effective two-dimensional rotationally adiabatic potential energy surfaces where p H₂ and o H₂ are point-like particles. These potentials for the H₂-X₂ complexes have global and local minima for effective linear and T-shaped complexes, respectively, which are separated by 0.4-1.0 kJ/mol, where o H₂ binds stronger than p H₂ to X₂, due to higher alignment to minima structures of the 4D-pair potential. Further, we provide fits of an analytical function to the rotationally adiabatic potentials. © 2014 AIP Publishing LLC. [<http://dx.doi.org/10.1063/1.4892599>]

I. INTRODUCTION

Hydrogen is the lightest molecule, with a large rotational constant, and thus quantum effects govern the dynamics of the single molecule, its clusters and macroscopic phases.^{1,2} The hydrogen molecule forms two nuclear spin isomers referred to as para- (p H₂) and ortho-hydrogen (o H₂). For hydrogen molecules in the electronic ground state, the antisymmetry principle states that p H₂ has rotational states with even main rotational quantum numbers, while for o H₂ only the odd numbered states are allowed. The resulting differences in the rotational energies lead in turn to differences in the macroscopic properties allowing, for example, the separation of para- from ortho-hydrogen. Due to the low mass, also the translation and vibration of H₂ molecules are subject to quantum effects. Theoretical investigations suggest that small clusters of parahydrogen ($(p$ H₂)_N) are liquid below 14 K, the melting point of bulk p H₂, and exhibit superfluid behaviour at temperatures below 1 K.³⁻⁶ The relative cluster stability is predicted to increase for clusters with N equal to icosahedral cluster magic numbers.^{7,8} Para-hydrogen crystals are translational quantum solids, where, due to the zero point energy, the hcp- is preferred over the fcc-lattice at low temperatures.^{2,9-11}

These quantum effects also have to be considered for H₂ clusters and solids doped with other molecules.¹²⁻¹⁴ For example, small p H₂ clusters show superfluid responses to ro-

tations of embedded OCS,¹⁵⁻¹⁷ CO₂,¹⁸ and CO¹⁹ molecules. Theoretical investigations rely on the respective pair potentials for the interaction of the dopant with H₂. This poses challenges for *ab initio* electronic structure calculations, as the interaction of H₂ with other closed shell molecules is in the order of only a few kJ/mol.²⁰⁻²² Therefore, accurate results are currently accessible only for systems with a small number of electrons. Similarly weak interactions are also known for rare-gas halogen systems, which have been studied extensively.²³⁻²⁷ In contrast to rare-gas matrices, halogens trapped in solid p H₂ can react with the matrix itself. Concerning the hydrogen halogen H₂X₂ systems, with X = F, Cl, and Br, the *ab initio* interactions of the (HX)₂ dimers²⁸⁻³² and of the atom-molecule pairs X-H₂³³⁻³⁶ have been studied in view of hydrogen bonding and the hydrogen halogen reaction. However, with the exceptions of H₂-I₂^{37,38} and H₂-F₂,³⁹ no reports about pair potentials for the H₂-X₂ dimers could be found in the literature. These potentials are important to understand the properties of hydrogen halogen mixtures prior to reaction. An example are the experiments by Kettwich *et al.*⁴⁰ who performed flash photolysis of Cl₂ diluted in p H₂ at cryogenic temperatures. The simultaneous irradiation with IR light, exciting p H₂ to the first vibrational state, lead to a significant increase in the yield of HCl, as was proposed by Korolkov *et al.*⁴¹ To model the quantum reaction dynamics of the photolysis of X₂ in a p H₂ matrix, an assumption about the orientation of X₂ and translation of H₂ within the crystal lattice has to be made.⁴¹ Here, the H₂-X₂ potentials are needed to construct the many body potentials for which the librational ground state wave functions answer these questions.^{42,43}

^{a)}m.berg@fu-berlin.de

^{b)}antonioaccardi80@gmail.com

^{c)}b.paulus@fu-berlin.de

^{d)}burkhard.schmidt@fu-berlin.de

One can in a good approximation adiabatically the pair potentials with respect to, not only the electronic and vibrational degrees of freedom, but also to the rotation of H_2 , as the rotational constant of H_2 is much larger than for the heavier halogen molecules. This reduces the four-dimensional (4D) pair potential to effective two-dimensional (2D) potentials for pH_2 and oH_2 , which facilitates studies of ensembles.⁴⁴ In particular, model functions developed for the quantum dynamics of diatomic molecules trapped in rare gas clusters^{45–52} can be readily applied. Developed for rare gas pair potentials, analytic Hartree-Fock-dispersion (HFD) models⁵³ are also suited to parametrize p/oH_2 interactions.^{21,54} Accurate intermolecular potentials for simple van der Waals complexes can also help in the development of on top dispersion corrections and atom-atom potentials used in molecular dynamics.

In view of the similarities of pH_2 to the rare gas atoms, it is interesting to compare their respective interaction potentials with halogen molecules. The rare gas atom- X_2 pair potentials are weakly anisotropic. Similar binding energies for linear and T-shaped complexes have been predicted by high level *ab initio* calculations^{23,25,26} and have been measured using laser-induced fluorescence and two-color action spectroscopy,^{55–57} see Ref. 58 for a review. We further compare the p/oH_2-X_2 interactions with those of pH_2 with other small molecules.

II. AB INITIO PAIR POTENTIALS

A. Methods

We assume the molecular wave function of the H_2-X_2 dimers to be approximately adiabatic with respect to the electronic ground state of the dimer, as well as to the vibrational ground state of the free monomers, i.e., we apply the Born-Oppenheimer and fixed monomer approximation. In the latter, the bond lengths of the monomers are kept constant at the following values $r_{H_2} = 75.7$ pm, $r_{F_2} = 141.2$ pm, $r_{Cl_2} = 203.3$ pm, and $r_{Br_2} = 228.1$ pm. The interaction energy then depends on the Jacobi coordinates of the systems, see Fig. 1, hence the distance R between the centers of mass of H_2 and X_2 , the polar θ_{H_2} , θ_{X_2} , and dihedral angles $(\phi_{H_2} - \phi_{X_2})$.

The interaction between non-polar molecules is governed by dispersion and electrostatic quadrupole-quadrupole (QQ) interactions. The former ones are roughly proportional to the polarizabilities of the molecules.⁵⁹ For H_2-X_2 , they are in the few kJ/mol regime, calling for highly accurate wave function based correlation methods, such as full configuration interaction (FCI), coupled cluster with singles and doubles and perturbative triples (CCSD(T)), and symmetry adapted perturbation theory (SAPT), in conjunction with large one electron basis sets.^{60,61}

Here, the interaction energies $\Delta E(R, \theta_{X_2}, \theta_{H_2}, \phi_{H_2} - \phi_{X_2})$, defined by

$$\Delta E = E(H_2X_2) - (E(X_2) + E(H_2)), \quad (1)$$

were calculated at the Møller-Plesset perturbation theory of second order (MP2) and CCSD(T) level of theories as implemented in the MOLPRO package of programs.^{62–64} For H, F, and Cl all electron aug-cc-pVnZ basis sets⁶⁵ (AVnZ) up to

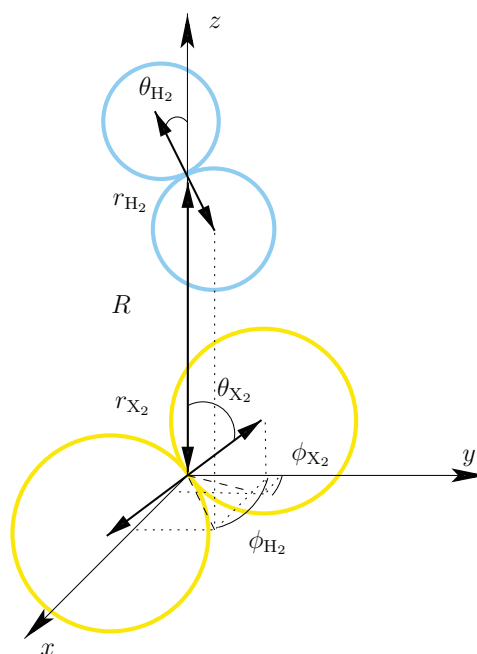


FIG. 1. Laboratory frame and internal coordinates. The halogen molecule (X_2) and the hydrogen molecule (H_2) are depicted by yellow and blue pairs of circles, respectively.

$n = 6$ (H, F) and $n = 5$ (Cl) were used. For Br the scalar-relativistic effective core potential ECP10MDF⁶⁶ was used in conjunction with the adapted aug-cc-pVnZ basis sets⁶⁶ up to $n = 5$. All interaction energies are corrected for the basis set superposition error via the counterpoise scheme.⁶⁷ Results referring to the complete basis set (CBS) limit are extrapolated from the results of the largest and second largest basis.⁶⁰ In the determination of the correlation energy virtual excitations were restricted to the valence electrons. Total energies are converged to a threshold of 10^{-8} Hartree.

B. CCSD(T) results

For the six structures of high symmetry, depicted in Fig. 2, $\Delta E(R)$ was calculated up to the CCSD(T)/CBS level of theory. The orientations are abbreviated by (a) letters T , H , and X forming similar shapes as the complexes and (b) by letters L and S which abbreviate the descriptions, “linear” and “slipped-parallel,” of the structures. We further discern the structures T for the H_2-X_2 pairs, where H_2 forms either the stem ($T1$) or the hat ($T2$). The minima of the CCSD(T) curves, obtained by spline interpolation, as well as curves from MP2/AVQZ are given in Fig. 3. Tabulated values are given in the supplementary material.⁶⁸ Trends within the CCSD(T)/CBS interaction energies are similar for all hydrogen-halogen pairs. The most strongly bound orientation is always $T2$, with well depths D_e increasing by about 1 kJ/mol in the order $F_2 < Cl_2 < Br_2$, and range from 1.3 over 2.4 to 3.2 kJ/mol. The least bound orientation of the six is always the linear one (L) with minimal interaction energies of -0.25 , -0.5 , and -0.6 kJ/mol for F_2 , Cl_2 , and Br_2 , respectively, where the minima occur at the largest monomer separation. Intermediate interaction energies are found for the

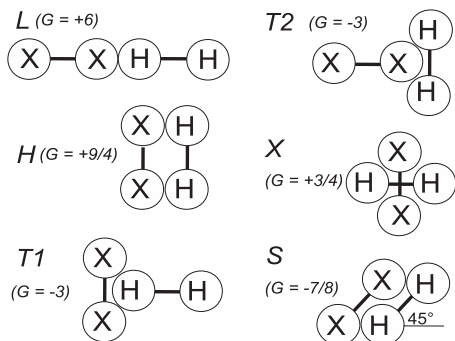


FIG. 2. Selected symmetric structures of H_2-X_2 pairs. The H -, $T1$ -, $T2$ -, and X -configurations take their names from their geometrical arrangements, whereas L and S stands for “linear” and “slipped parallel,” respectively. The corresponding geometrical factors G in Eq. (3) for the quadrupole-quadrupole interaction are given in brackets.

$T1$, X , H , and S structures. For all three systems, the minima of $T1$, X , H are found at the smallest monomer separations and are similar in energy. Within this group, the absolute interaction energy decreases from $T1$ over H to X . While for Cl_2 and Br_2 the interaction energy of H is closer to that of $T1$ than the one of X , for F_2 the interaction energies of H and X are closest instead. The minimum of the $\Delta E(R)$ curves of the S orientation is found at distances between the minima of the $T2$ and L curves. For Cl_2 and Br_2 , the respective absolute interaction energy is always below that of the $T1$, H , X group, while for F_2 , it is in between the close values for H and X .

To emphasize the anisotropy of the hydrogen-halogen molecular interaction, we included the hydrogen-hydrogen CCSD(T)/AV5Z molecular pair potentials at equivalent orientations in Fig. 3. For this system, the orientations $T1$ and $T2$ degenerate to T , with a well depth of 0.43 kJ/mol. Thus, the interaction of H_2 with H_2 is 3, 5.6, and 7.5 times weaker than with F_2 , Cl_2 , and Br_2 , respectively. In contrast to the interaction with halogen molecules, structure S and T are very close in energy, differing by only 0.03 kJ/mol. Note also the similarity of the interaction energies for X and H to the L orientation. Hence, the H_2-H_2 pair interaction is much more isotropic and weaker, in comparison to the hydrogen halogen pair interactions.

C. Electrostatic contributions

In this subsection, we want to illustrate in how far the interaction energy can be associated to electrostatic forces. While a rigorous approach to quantify all separate types of interactions would involve SAPT theory,⁶¹ we restrict ourselves to calculate only the electrostatic QQ interaction to obtain at least a qualitative measure for their importance. Because the quadrupole moments are the lowest non-vanishing multipole moments for linear neutral homonuclear molecules. Hence, their interaction is the leading term of the multipole expansion for the electrostatic interaction, which is given by⁵⁹

$$U_{Q_{X_2} Q_{H_2}}(R) = \frac{Q_{X_2} Q_{H_2}}{4\pi\epsilon_0 R^5} \times G(\theta_{X_2}, \theta_{H_2}, \phi_{H_2} - \phi_{X_2}). \quad (2)$$

The components of the quadrupole tensors along the bond axis are $Q_{H_2} = 0.4252 ea_0^2$, $Q_{F_2} = 0.7635 ea_0^2$,

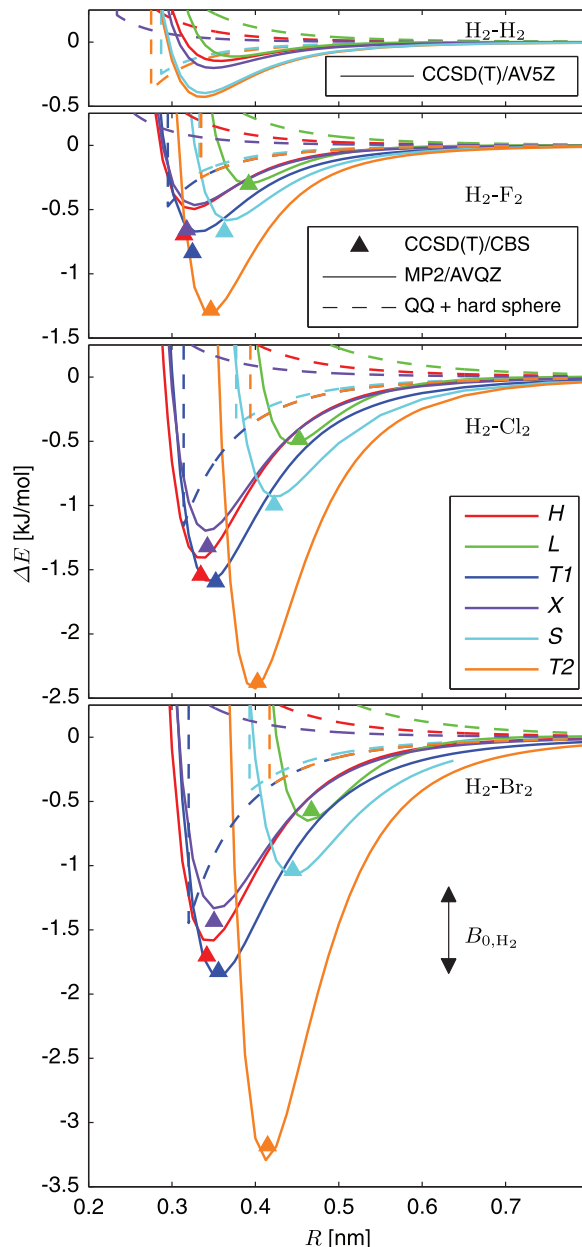


FIG. 3. Interaction energies ΔE between H_2 and H_2 , F_2 , Cl_2 , and Br_2 for the static orientations shown in Fig. 2. *Ab initio* results (full lines) for H_2-H_2 are calculated at the CCSD(T)/AV5Z level of theory. The interactions of H_2 with the halogens, denoted by full lines, are of MP2/(H,F,Cl: AVQZ, Br: $\dot{E}CP10MDF$ AVQZ) quality. Triangles at the maximal CCSD(T)/CBS binding interactions are included as reference points to judge the accuracy of the MP2 results. Dashed lines show hard sphere quadrupole-quadrupole model interactions.

$Q_{Cl_2} = 2.5427 ea_0^2$, $Q_{Br_2} = 0.7635 ea_0^2$, calculated at the CCSD(T)/AV6Z, MP2/AV6Z, MP2/AV6Z, and MP2/AV5Z levels of theory, respectively. The geometrical factor G is given by

$$G(\theta_{X_2}, \theta_{H_2}, \phi_{H_2} - \phi_{X_2}) = \frac{3}{4} \{ 1 - 5 \cos^2 \theta_{X_2} - 5 \cos^2 \theta_{H_2} - 15 \cos^2 \theta_{X_2} \cos^2 \theta_{H_2} + 2[4 \cos \theta_{X_2} \cos \theta_{H_2} - \sin \theta_{X_2} \sin \theta_{H_2} \cos(\phi_{H_2} - \phi_{X_2})]^2 \}. \quad (3)$$

The values of G for the six orientations discussed above are also given in Fig. 2. We truncate $U_{Q_{X_2} Q_{H_2}}(R)$ at the contact distances given by a very simple “hard-sphere” (HS) model, where the atoms are represented by hard spheres with van der Waals radii of 110 pm, 147 pm, 175 pm, and 185 pm for the H, F, Cl, and Br atoms, respectively.⁶⁹

The corresponding QQ+HS interactions $U_{Q_{X_2} Q_{H_2}}$, are depicted in Fig. 3 by dashed lines. For the H_2 - H_2 complex, this model predicts, in accordance with the results from the electronic structure calculations, structure T as the most stable followed by structure S . The QQ+HS interactions for X , H , L are repulsive, thus these complexes are bound only due to dispersion forces. The latter also holds for the H_2 - X_2 pairs. Here, bonding electrostatic contributions are present for $T1$, $T2$, and S . In the QQ+HS model, the only difference between $T1$ and $T2$ is the HS contact distance. The $T1$ interaction energy has the highest QQ contribution followed by S and $T2$. From this we deduce, that H_2 - X_2 structures $T2$ are highly stabilized by dispersion interactions, while for $T1$ structures the QQ and dispersion interactions are approximately equal in magnitude. Thus, it is unsurprising that, when comparing F_2 , Cl_2 , and Br_2 , the changes in the QQ interactions are too small to account for the increase in the $T2$ well depth in this series. On the other hand, for $T1$ the QQ+HS interactions very well describe the actual changes in the interaction energy.

D. MP2 results

A large number of *ab initio* calculations are needed to get a fine angular and spatial resolution for the potential energy hypersurfaces $\Delta E(R, \theta_{X_2}, \theta_{H_2}, \phi_{H_2} - \phi_{X_2})$. Hence, due to economical reasons we have to resort to the MP2 method in their evaluation, unless symmetry allows otherwise. In the following part, we therefore compare the CCSD(T)/CBS results to those obtained at the MP2 level of theory. Fig. 3 shows full curves for the R dependence of the MP2/AVQZ interaction energy of dimers in fixed orientations and for comparison the location of CCSD(T)/CBS minima. Tables holding the respective R_e and D_e are provided in the supplementary material.⁶⁸ The CCSD(T)/CBS binding distances R_e are well recovered by MP2/AVQZ. Averaging the absolute deviations for D_e from MP2/AVQZ calculations, with respect to the CCSD(T)/CBS values, for the six test structures of each complex, yields 0.11 kJ/mol for H_2 - F_2 , 0.07 kJ/mol for H_2 - Cl_2 , and 0.09 kJ/mol for H_2 - Br_2 . In terms of absolute relative deviations, the mean values are 15%, 6%, and 7% for the complexes with F_2 , Cl_2 , and Br_2 , respectively. Thus, on average MP2/AVQZ performs better for H_2 - Cl_2 and H_2 - Br_2 than for H_2 - F_2 . We also tested larger basis sets of $n = 5, 6$ quality with the result, see Fig. 4, that the mean absolute relative deviations do not change. Basis sets with $n = 3$, however, increase the deviations considerably, as tested for F_2 and Br_2 .

Next, we compare the performance of MP2/AVQZ for each of the orientations individually. The global minima, i.e., well depths of $T2$, are in excellent agreement with the CCSD(T)/CBS results, for all three complexes, as $\Delta D_e(T2)$ ranges from -0.03 kJ/mol (H_2 - F_2) to -0.07 kJ/mol (H_2 -

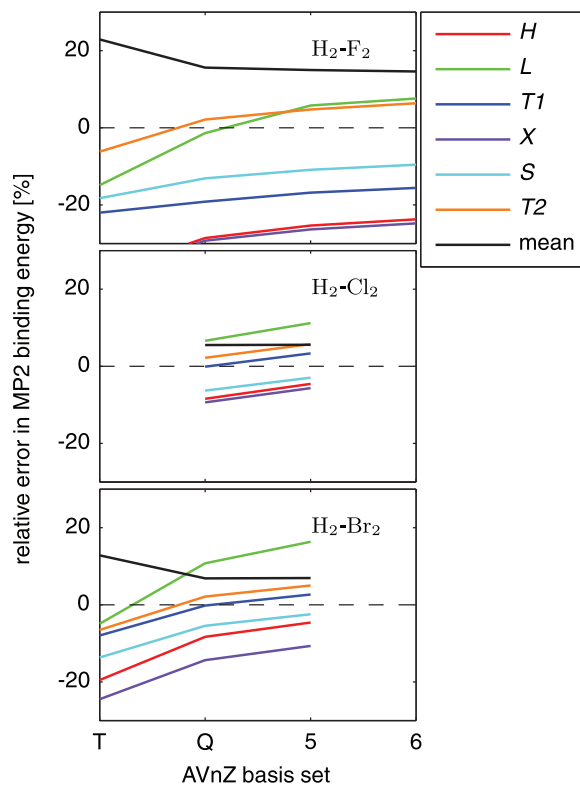


FIG. 4. Basis set dependence of relative deviations of MP2 well depths D_e with respect to CCSD(T)/CBS values for the structures shown in Fig. 2.

Br_2). The MP2/AVQZ well depths for the S , L , and $T1$ structures of the H_2 complexes with Cl_2 , Br_2 agree similarly well ($|\Delta D_e| < 0.1$ kJ/mol) with the CCSD(T)/CBS reference data. For H_2 - F_2 , the well depths of L and S are also within 0.1 kJ/mol of the CCSD(T)/CBS values. However, the well depth of the $T1$ structure of H_2 - F_2 is underestimated by 0.16 kJ/mol, which is a considerable deviation from the MP2/AVQZ errors $\Delta D_e(T1)$ of only 0.002 kJ/mol and 0.003 kJ/mol for the H_2 - Cl_2 and H_2 - Br_2 complexes. The least agreement is found for the X and H structures of all complexes, where MP2/AVQZ systematically underestimates well depths by 0.13 kJ/mol-0.22 kJ/mol. However, the energetic ordering remains the same as with CCSD(T)/CBS. This also holds for all tested structures with the exception of the H , X , and S structures of H_2 - F_2 . Here, the CCSD(T)/CBS well depths are within a range of just 0.04 kJ/mol and are ordered $H > S > X$, whereas with MP2/AVQZ the ordering changes to $S > H > X$. Overall, the MP2/AVQZ method performs very well for H_2 - Cl_2 and H_2 - Br_2 , while anisotropies with respect to the H and X structures are slightly overestimated. The pair potential of H_2 - F_2 is less anisotropic in comparison, thus the MP2 errors, although similar in magnitudes, lead to a less accurate description of the potential. In particular, anisotropies of the H_2 - F_2 pair potential with respect to the H , L , and $T1$ structures are overestimated by MP2. In summary, the MP2/AVQZ method presents an economic way to describe the interaction energy reasonably well for the six structures for all investigated complexes within the discussed limits.

III. ROTATIONALLY ADIABATIC (RA) POTENTIAL ENERGY SURFACE

A. Method

Because the rotational constant of H₂ is 62, 244, and 724 times larger than the rotational constants of ¹⁹F₂, ³⁵Cl₂, and ⁷⁹Br₂, it is a justified approximation, to adiabatically the pair potentials with respect to the rotational degrees of freedom of H₂. This yields two-dimensional potentials, depending on the orientation of the halogen molecule and the distance *R*, which is equivalent to an effective point-like H₂ molecule representing a certain rotational state. In most of the previous work found in the literature,^{70–74} effects of H₂ rotation are eliminated by considering the free rotor ground state only, i.e., by isotropic averaging with respect to the rotational degrees of freedom. In this approximation, perturbations of the free rotor states due to the presence of an intermolecular potential are neglected. Li *et al.* have compared isotropic averaging with the “adiabatic-hindered-rotor” treatment, for *p*H₂–CO, *p*H₂–CO₂, and *p*H₂–*p*H₂. They concluded, that the latter method results in more accurate binding energies and spectra over the former.⁴⁴ Considering that the binding energies of the H₂–X₂ complexes, see Fig. 3, are up to 2, 3.5, and 4.7 times larger than the rotational constant of H₂, we have to expect a hindered rotation around the global minima. Consequently, we employ the “adiabatic-hindered-rotor” method, i.e., we calculate RA pair potentials, by solving the rotational Schrödinger equations (SE)

$$\begin{aligned} \hat{H}_{\text{rot}}(\theta_{\text{H}_2}, \phi_{\text{H}_2}; R, \theta_{\text{X}_2}, \phi_{\text{X}_2})\Psi_n(\theta_{\text{H}_2}, \phi_{\text{H}_2}; R, \theta_{\text{X}_2}, \phi_{\text{X}_2}) \\ = W_n(R, \theta_{\text{X}_2}, \phi_{\text{X}_2})\Psi_n(\theta_{\text{H}_2}, \phi_{\text{H}_2}; R, \theta_{\text{X}_2}, \phi_{\text{X}_2}), \end{aligned} \quad (4)$$

in the variables θ_{H_2} and ϕ_{H_2} , which are separated from the parameters R , θ_{X_2} , and ϕ_{X_2} by the semicolon. The Hamiltonians for the rotation of rigid H₂ in the H₂–X₂ complex are

$$\begin{aligned} \hat{H}_{\text{rot}}(\theta_{\text{H}_2}, \phi_{\text{H}_2}; R, \theta_{\text{X}_2}, \phi_{\text{X}_2}) \\ = B_0 \hat{J}_{\text{H}_2}^2 + \Delta E(R, \theta_{\text{X}_2}, \theta_{\text{H}_2}, \phi_{\text{H}_2} - \phi_{\text{X}_2}), \end{aligned} \quad (5)$$

where $B_0 = 0.6812$ kJ/mol is the rotational constant of the hydrogen molecule in the vibrational ground state, and \hat{J}_{H_2} is the corresponding angular momentum operator. The second term ΔE denotes the respective H₂–X₂ pair potential from quantum chemistry MP2/AVQZ or CCSD(T)/AVQZ calculations, see Sec. II. Equation (4) is solved using a representation in a basis of spherical harmonics $Y_{JM}(\theta_{\text{H}_2}, \phi_{\text{H}_2})$, where the potential energy matrix elements

$$\begin{aligned} \Delta E_{J'M'JM}(R, \theta_{\text{X}_2}, \phi_{\text{X}_2}) \\ = \frac{1}{4\pi} \int_1^{-1} d \cos \theta_{\text{H}_2} \int_0^{2\pi} d\phi_{\text{H}_2} \\ \times \Delta E(R, \theta_{\text{X}_2}, \theta_{\text{H}_2}, \phi_{\text{H}_2} - \phi_{\text{X}_2}) \\ \times Y_{J'M'}^*(\theta_{\text{H}_2}, \phi_{\text{H}_2}) Y_{JM}(\theta_{\text{H}_2}, \phi_{\text{H}_2}) \end{aligned} \quad (6)$$

$$\begin{aligned} \approx \frac{1}{4\pi} \sum_{k=1}^8 w_k \sum_{j=1}^{16} w_j \\ \times \Delta E(R, \theta_{\text{X}_2}, \theta_{\text{H}_2,k}, \phi_{\text{H}_2,j} - \phi_{\text{X}_2}) \\ \times Y_{J'M'}^*(\theta_{\text{H}_2,k}, \phi_{\text{H}_2,j}) Y_{JM}(\theta_{\text{H}_2,k}, \phi_{\text{H}_2,j}), \end{aligned} \quad (7)$$

are approximately computed by means of a Gaussian quadrature, involving the weights w_k and w_j , which implies the *ab initio* PESs, ΔE , to be evaluated at some definite Gauss–Legendre grid-points $\theta_{\text{H}_2,k}$ and $\phi_{\text{H}_2,j}$, with ϕ_{X_2} held constant. The pair potentials ΔE subject to the rotational adiabaticization are calculated using the following fixed bond lengths, $r_{\text{H}_2} = 76.7$ pm, $r_{\text{F}_2} = 141.7$ pm, $r_{\text{Cl}_2} = 203.3$ pm, and $r_{\text{Br}_2} = 228.1$ pm, which correspond to vibrational ground state averages. For each point (R, θ_{X_2}) the pair potential ΔE represented by a 16×8 Gauss–Legendre grid over $\theta_{\text{H}_2,k}$ and $\phi_{\text{H}_2,j}$ was calculated at the MP2/AVQZ level of theory, with $\phi_{\text{X}_2} = 45^\circ$. This 16×8 grid assures the first four eigenvectors to be well converged, for details see Ref. 8. We performed linear scans over θ_{X_2} , ranging from 0° to 90° , with an increment of 5° . For each value of θ_{X_2} , a varying number of monomer separations R , were evaluated. The smallest increment used in the R direction was 10 pm. Collectively, the ΔE contain 50 176, 87 552, and 41 600 individual structures for H₂–F₂, H₂–Cl₂, and H₂–Br₂, respectively. For $\theta_{\text{X}_2} = 0^\circ$, ΔE is of cylindrical symmetry, thus independent of ϕ_{H_2} , which reduces the number of non-equivalent Gauss–Legendre points from 128 to 8. When $\theta_{\text{X}_2} = 90^\circ$ the potential has C_{2v} symmetry, hence it is sufficient to evaluate one quarter of the sphere, which means 32 points in our case. Exploiting these symmetries, we also performed CCSD(T)/AVQZ level of theory scans along R for $\theta_{\text{X}_2} = 0^\circ$ and $\theta_{\text{X}_2} = 90^\circ$. Files containing all calculated points are provided in the supplementary material.⁶⁸

The first eigenvector of Eq. (4), Ψ_0 is asymptotically ($R \rightarrow \infty$) correlated with the free rotor state with $J = 0$, thus it is the rotational ground state wave function of *p*H₂ in the H₂–X₂ complex, to which belongs the RA potential $W_0(R, \theta_{\text{X}_2})$. Likewise, the next three states Ψ_1 , Ψ_2 , and Ψ_3 are asymptotically correlated with the free rotor states of *o*H₂, with quantum numbers $J = 1$, ($M = -1, 0, 1$). Their corresponding eigenvalues $W_n(R, \theta_{\text{X}_2})$ define the RA potentials for *o*H₂. For the linear complex ($\theta_{\text{X}_2} = 0^\circ$), the first two *o*H₂ states are degenerate and separated from the third state, hence $W_1(R, 0^\circ) = W_2(R, 0^\circ) < W_3(R, 0^\circ)$.

At large separations R , $W_0(R, \theta_{\text{X}_2})$ converges to zero for the free *p*H₂, while $W_{1-3}(R, \theta_{\text{X}_2})$ converge to the rotational energy $2B_0$ of free *o*H₂. The interaction energies ΔW for the complexes are given by $\Delta W_0(R, \theta_{\text{X}_2}) = W_0(R, \theta_{\text{X}_2})$ for *p*H₂ and $\Delta W_{1-3}(R, \theta_{\text{X}_2}) = W_{1-3}(R, \theta_{\text{X}_2}) - 2B_0$ for *o*H₂.

B. Nuclear spin effect

Before we discuss the features of the RA pair potentials for the interaction energy ΔW_0 and ΔW_1 for *p*H₂–X₂ and *o*H₂–X₂ in detail, see Sec. III D, we compare the probability

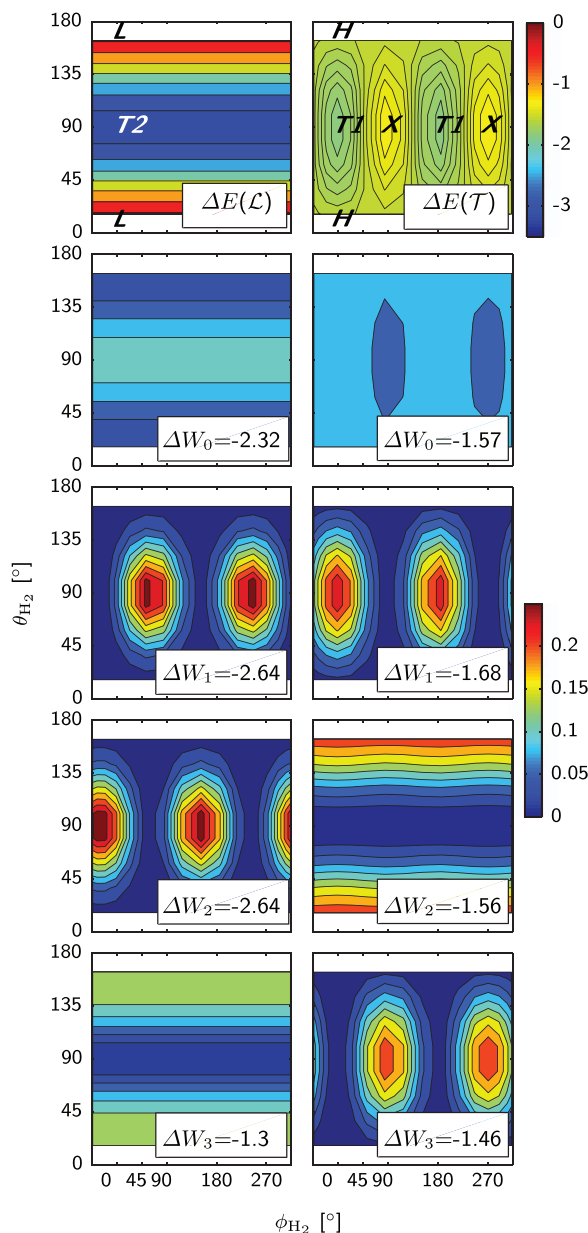


FIG. 5. Potentials for $\text{H}_2\text{-Br}_2$ at the MP2/AVQZ level of theory (1st row, in kJ/mol) and the rotational densities for $p\text{H}_2$ (2nd row) and $o\text{H}_2$ (3rd-5th row), in the linear minimum (left panel, $\theta_{\text{Br}_2} = 0^\circ$, $R = 420$ pm) and the T-shape minimum (right panel, $\theta_{\text{Br}_2} = 90^\circ$, $R = 354$ pm) of the RA potential of $\text{H}_2\text{-Br}_2$. The position of high symmetry structures is indicated by $T1, T2, \dots$, see Fig. 2.

distributions $|\Psi_n|^2$, effective interactions ΔW_n , and the perturbing potentials ΔE for the first four rotational eigenstates of H_2 exemplarily for the $\text{H}_2\text{-Br}_2$ system. We do so for two points (R, θ_{Br_2}) close to the global and local minima of the RA potentials ΔW_n . We choose $\text{H}_2\text{-Br}_2$ because the respective pair interaction is stronger than for F_2 and Cl_2 , and thus perturbations to the free rotor states of H_2 are more pronounced.

The coordinates $R = 420$ pm, $\theta_{\text{Br}_2} = 0^\circ$ are close to the global minima, i.e., the linear case, of the $p\text{H}_2\text{-Br}_2$ RA potential, see Sec. III D. Here, the part of the 4D pair potential $\Delta E(\mathcal{L}) = \Delta E(420 \text{ pm}, 0^\circ, \theta_{\text{H}_2}, \phi_{\text{H}_2} - 45^\circ)$, given in the top left panel of Fig. 5, depends only on θ_{H_2} . The minimum of

the static $T2$ structure at $\theta_{\text{H}_2} = 90^\circ$ dominates the interaction, which becomes weaker approaching the unfavourable limit of the static L structure at $\theta_{\text{H}_2} = 0^\circ$ and $\theta_{\text{H}_2} = 180^\circ$. The distribution of $|\Psi_0|^2$ is notably perturbed by the potential, i.e., the ground state of $p\text{H}_2$ is not spherical. Instead, it is more aligned to the static $T2$ structure and thereby less to the L structure. Hence, the isotropic averaging approximation would underestimate the binding interaction of $p\text{H}_2\text{-Br}_2$. The free $o\text{H}_2$ molecule has a triply degenerate rotational ground state. In the effective linear complex, this degeneracy is partly lifted. The lowest two $o\text{H}_2$ eigenstates Ψ_1, Ψ_2 are degenerate and aligned to the static $T2$ structure, with two nodes along $\phi(\text{H}_2)$. As this alignment to the strongly bound $T2$ structure is more pronounced for $o\text{H}_2$, it also interacts stronger with Br_2 than $p\text{H}_2$. Note that this comes at the cost of an increase in kinetic energy by $2B_0$ for $o\text{H}_2$ over $p\text{H}_2$. The third $o\text{H}_2$ eigenstate Ψ_3 is aligned to the static L structure and thus lies well above the first two states.

The energetic ordering of the rotational states at the T-shape local minimum, see right panel of Fig. 5, can be explained by the potential $\Delta E(T) = \Delta E(354 \text{ pm}, 90^\circ, \theta_{\text{H}_2}, \phi_{\text{H}_2} - 45^\circ)$. First, it is energetically more isotropic than $\Delta E(\mathcal{L})$ as the interaction energies of the static $T1, H$, and X structures are similar at this intermolecular separation. Hence, interaction energies of the rotational states are closer together as well. Consequently, the para/ortho splitting is expected to be smaller. Second, the interaction is weaker than for the linear-shaped case. Thus, the perturbation with respect to the free rotor states is lower, as can be seen in the very isotropic distribution $|\Psi_0|^2$. Third, the potential depends on both rotational degrees of freedom, ϕ_{H_2} and θ_{H_2} , of H_2 , which lifts the degeneracy of the free $o\text{H}_2$ ground state. The $p\text{H}_2$ density stays approximately spherically symmetric, since its alignment to the $T1$ structure would imply a node in the wave function, a mixing of higher angular momentum states, that would require kinetic energies in the order of $6B_0$. For $o\text{H}_2$, we find that $|\Psi_1|^2$ essentially aligns to the $T1$, $|\Psi_2|^2$ with the H , and $|\Psi_3|^2$ with the X structure, which are energetically most, second, and least favoured. In summary, for the T-shaped complexes the alignment of $o\text{H}_2$ to the $T1$ structure leads to a larger binding interaction in comparison to $p\text{H}_2$.

C. Fit to analytic function

Analytic expressions of potentials facilitate the future use in simulations. The rotationally adiabatic MP2 pair potentials ΔW_n were fitted to a modified HFD function⁵³

$$\Delta W_n(R, \theta_{X_2}) = a(\theta_{X_2}) \exp[-b(\theta_{X_2})R] - S(R) \left(\frac{C_6(\theta_{X_2})}{R^6} + \frac{C_8(\theta_{X_2})}{R^8} \right), \quad (8)$$

where the first term represents the Pauli repulsion interaction and the second term the dispersion interaction. The dispersion

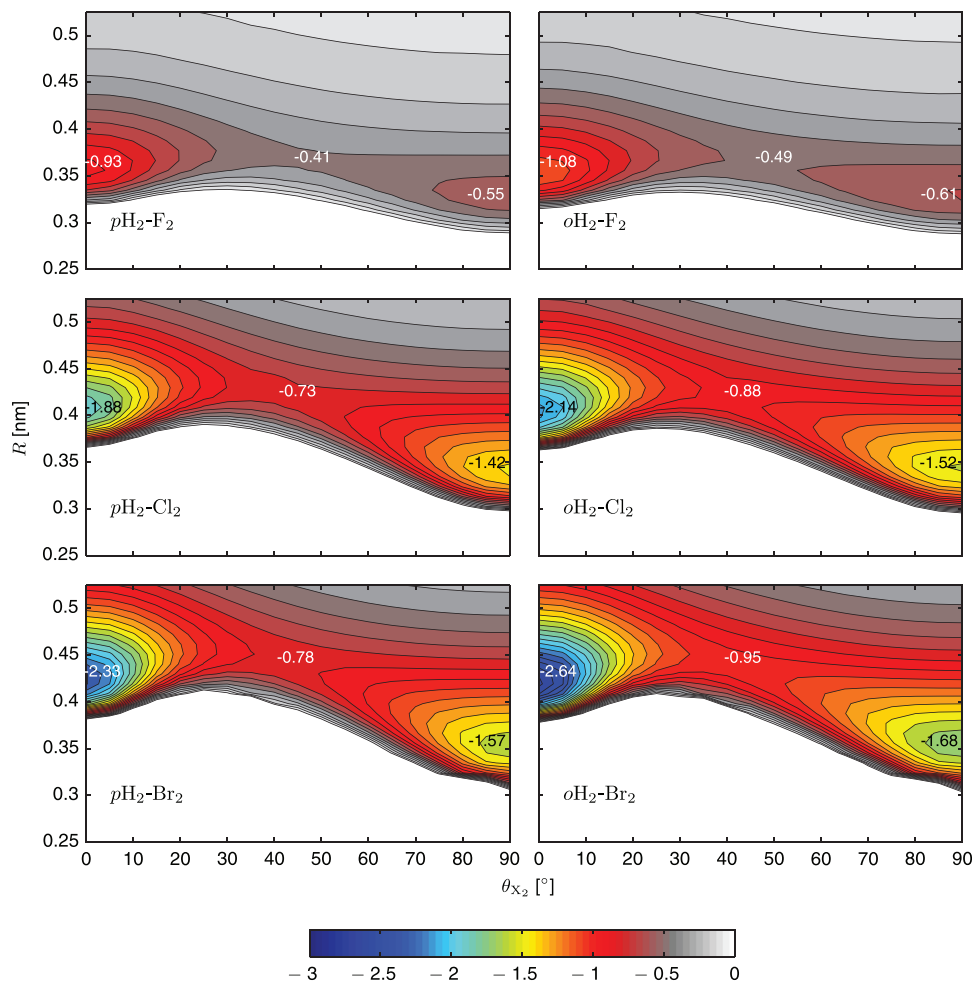


FIG. 6. Rotationally adiabatic MP2/AVQZ potentials for the interaction ΔW of para- and ortho-hydrogen, in their rotational ground states, with fluorine, chlorine, and bromine molecules. Contour levels for ΔW , ranging from -3 to 0 kJ/mol, are shown at 0.1 kJ/mol increments.

decays algebraically, hence a switching function

$$S(R) = \begin{cases} \exp[-(1.28R_e(0^\circ)/R - 1)^2], & \text{if } R \leq 1.28R_e(0^\circ), \\ 1, & \text{if } R \geq 1.28R_e(0^\circ), \end{cases} \quad (9)$$

which truncates the dispersion energy toward short internuclear distances, becomes necessary. We have simplified the original HFD function, by omitting the R^2 dependence in the repulsion exponent and the R^{-10} dependence of the dispersion, since 1D cuts of the potentials for fixed θ_{X_2} , could be reproduced to good accuracy without them. We further decided to omit the angular dependence of the switching function S , by making it only dependent on the position $R_e(0^\circ)$ of the global minimum of the pH_2-X_2 potential. The angular dependence of the other fitting parameters a , b , C_6 , and C_8 is expanded in terms of the first six even-ordered Legendre polynomials P_{2k} ,

$$X(\theta_{X_2}) = \sum_{k=0}^5 X_{2k} P_{2k}(\cos \theta_{X_2}), \quad (10)$$

where X_0 to X_{10} are the corresponding expansion coefficients. Our 2D HFD fits reproduce the global minima with maximal deviations of 2%. Tabulated fit results and original data points are provided in the supplementary material.⁶⁸

D. Potential energy surfaces for the interaction of pH_2 and oH_2 with X_2

The rotationally adiabatic pair potentials for the interaction energy, ΔW , of the p/oH_2-X_2 dimers for the rotational ground states of pH_2 and oH_2 have two minima. The respective contour plots, representing the results obtained from the MP2/AVQZ calculations, are given in Fig. 6, for minimum energy paths we refer to Fig. 7. Equilibrium distances and well depths for both minima are provided in Table I. These have been obtained for cuts of the potentials along $\theta_{X_2} = 0^\circ$

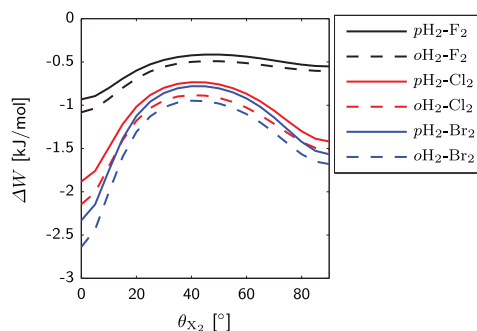


FIG. 7. Minimum MP2/AVQZ interaction energy angular paths for para- and ortho-hydrogen, in their rotational ground states, with fluorine, chlorine, and bromine molecules.

TABLE I. *Ab initio* well depths D_e [kJ/mol] and equilibrium distances R_e [pm] for the p/oH_2-X_2 and $Rg-X_2$ complexes with $X = F, Cl, Br$; $Rg = He, Ne, Ar$ as well as small molecules from the literature.

Complex	Ref.	Method	Linear ($\theta_{X_2} = 0^\circ$)		T-shape ($\theta_{X_2} = 90^\circ$)	
			D_e	R_e	D_e	R_e
pH_2-F_2	present work	CCSD(T)	0.845	361	0.678	322
		MP2	0.932	357	0.552	328
oH_2-F_2	present work	CCSD(T)	0.986	356	0.725	325
		MP2	1.081	353	0.606	330
$He-F_2$	25	CCSD(T)	0.429	347	0.382	300
$Ne-F_2$	25	CCSD(T)	0.736	359	0.735	308
$Ar-F_2$	25	CCSD(T)	1.469	388	1.316	344
pH_2-Cl_2	present work	CCSD(T)	1.686	412	1.390	343
		MP2	1.882	408	1.419	342
oH_2-Cl_2	present work	CCSD(T)	1.938	409	1.459	345
		MP2	2.144	404	1.518	343
$He-Cl_2$	23	MP4	0.481	420	0.449	345
$Ne-Cl_2$	23	MP4	0.973	427	0.925	350
$Ar-Cl_2$	23	CCSD(T)	2.572	448	2.524	374
pH_2-Br_2	present work	CCSD(T)	2.111	428	1.539	353
		MP2	2.330	424	1.567	352
oH_2-Br_2	present work	CCSD(T)	2.410	425	1.623	356
		MP2	2.638	421	1.682	354
$He-Br_2$	26	CCSD(T)	0.584	442	0.482	358
$Ne-Br_2$	26	CCSD(T)	1.120	449	0.805	360
$Ar-Br_2$	26	CCSD(T)	3.143	463	2.708	380

Complex	Ref.	Method	Linear				T-shape	
			D_e	R_e	D_e	R_e	D_e	R_e
pH_2-pH_2	44, 75	CCSD(T)	0.295	346				
pH_2-CO	44, 76	CCSD(T)	$\theta_1 = 0^\circ (C)$		$\theta_1 = 180^\circ (O)$		$\theta_1 = 85.8^\circ$	
			0.443	440	0.514	400	0.610	360
pH_2-CO_2	44, 78	CCSD(T)	$\theta_1 = 180^\circ$		$\theta_1 = 90.0^\circ$			
			0.667	444	1.340	319		
pH_2-N_2O	79	CCSD(T)	$\theta_1 = 0^\circ (N)$		$\theta_1 = 180^\circ (O)$		$\theta_1 = 92.58^\circ$	
			0.60	460	0.821	429	1.691	308
oH_2-N_2O	79		$\theta_1 = 0^\circ (N)$		$\theta_1 = 180^\circ$		$\theta_1 = 92.88^\circ$	
			0.86	460	1.02	430	2.09	302
pH_2-HCN	80, 81	CCSD(T)-F12a	$\theta = 0^\circ (H)$		$\theta = 180^\circ (N)$		$\theta \approx 60^\circ$	
		spherical average	≈ 0.66	410	0.948	430	0.750	407
pH_2-OCS	15, 77	MP4	$\theta = 0^\circ (S)$		$\theta = 180^\circ (O)$		$\theta = 105^\circ$	
		spherical average	1.093	452	0.828	492	1.729	335
pH_2-H_2O	22, 82	CCSD(T),	$\theta = 110.00^\circ, \chi = 0^\circ$					
		CCSD(T)-R12			1.167	336		

and $\theta_{X_2} = 90^\circ$, respectively. The global minima of ΔW correspond to linear ($\theta_{X_2} = 0^\circ$) p/oH_2-X_2 complexes, which is anticipated, since the underlying static 4D pair potential for ΔE for $\theta_{X_2} = 0^\circ$, see Secs. II and III B, involves the static global minima $T2$ structures. With ΔE calculated at the MP2/AVQZ level of theory, the minimum interaction energies ΔW for the linear complexes range from -0.93 kJ/mol for pH_2-F_2 to -2.64 kJ/mol for oH_2-Br_2 . The local minimum of each re-

spective potential ΔW , corresponds to T-shaped ($\theta_{X_2} = 90^\circ$) p/oH_2-X_2 complexes, where the averaging over ΔE includes mainly the static $T1$, H , and X structures. The interaction energies for the T-shaped complexes at the MP2/AVQZ level of theory range from -0.55 kJ/mol for pH_2-F_2 to -1.68 kJ/mol for oH_2-Br_2 . The anisotropy in the energy, i.e., the difference between global and local minima, ranges from 0.38 kJ/mol for pH_2-F_2 to 0.96 kJ/mol for oH_2-Br_2 . The energy values at the

saddle points, which are located in the vicinity of $\theta_{X_2} = 40^\circ$, range from -0.42 kJ/mol ($p\text{H}_2\text{-F}_2$) over -0.73 kJ/mol ($p\text{H}_2\text{-Cl}_2$) to -0.95 kJ/mol ($o\text{H}_2\text{-Br}_2$) with small para/ortho splittings of 0.07 kJ/mol, 0.10 kJ/mol, and 0.13 kJ/mol, for F_2 , Cl_2 , and Br_2 , respectively. For any given θ_{X_2} , the complexes with $o\text{H}_2$ are bound more strongly than those with $p\text{H}_2$, which can be explained in terms of a higher degree of alignment to more stable static structures for $o\text{H}_2$, see also Sec. III B. The rotationally adiabatic pair potentials with Cl_2 and Br_2 are more similar in comparison to ΔW with F_2 , as the potentials for $p/o\text{H}_2\text{-F}_2$ are significantly less anisotropic in terms of both energies and distances.

For both minima of the ΔW potentials, the respective CCSD(T)/AVQZ results, given in Table I, lead essentially to the same conclusions, as drawn from the MP2/AVQZ results. However, we find that the MP2 method overestimates the strength of the van der Waals bonds for the linear $p/o\text{H}_2\text{-X}_2$ complexes by 10%, in comparison to CCSD(T) results. For the T-shaped complexes of $p/o\text{H}_2$ with Cl_2 and Br_2 , MP2 overestimates the bonding interaction by 2%-5% and underestimates it for the T-shaped F_2 complexes by up to 19%. Thus, the $p/o\text{H}_2\text{-F}_2$ potentials are even less anisotropic than suggested by the MP2 results. While relative deviations up to 19% seem to be quite high, the corresponding absolute deviations are on the order of only hundredths to tenths of kJ/mol, due to the overall weakness of the interactions.

IV. CONCLUSIONS

We calculated the pair interaction of the hydrogen molecule with a fluorine, chlorine, and bromine molecule up to the CCSD(T) level of theory in the complete basis set limit. The highest binding interaction is present, for structure *T2*, where the molecular axis of the halogen molecule points perpendicular to the molecular axis of the hydrogen molecule. The second highest binding interaction belongs to structure *T1*, where the molecular axis of the hydrogen molecules points perpendicular to the molecular axis of the halogen molecule. A simple hard sphere model with quadrupole-quadrupole interactions underestimates the binding interaction globally and predicts the highest binding interaction for structure *T1*. As this model lacks any dispersion forces, the comparison with the quantum chemistry results confirms, that they are essential to describe the pair interaction of the $\text{H}_2\text{-X}_2$.

To investigate the interaction energy of $p\text{H}_2$ and $o\text{H}_2$ molecules with the halogen molecules, the pair potentials have been adiabaticized with respect to the rotational degrees of freedom of H_2 . The whole effective pair potentials have been calculated at the MP2/AVQZ level of theory, while for linear and T-shaped complexes additional CCSD(T)/AVQZ calculations could be performed. The global minimum structure is always a linear complex. Due to higher alignment to static low energy structures, the $o\text{H}_2\text{-X}_2$ complexes are more strongly bound than the respective $p\text{H}_2\text{-X}_2$ complexes. For bromine and chlorine, the MP2/AVQZ level of theory overestimates the well depths of the linear complex by up to 10%, and up to 5% for the T-shaped complex. For fluorine, the well depth of the T-shaped complex is underestimated by up to 19% at

the MP2/AVQZ level of theory. For future utilization of the effective potentials, we provide analytic fits to HDF model functions.

We are now in the position to compare the interactions of $p\text{H}_2$ and $o\text{H}_2$ with X_2 to the respective rare gas atom ($\text{Rg} = \text{He}, \text{Ne}, \text{and Ar}$) dihalogen interactions from the literature.^{23,25,26} Each of the Rg-X_2 2D pair potentials also has a global minimum for linear and a local minimum for T-shaped structures. However, the potentials are known for their low anisotropy, with similar energies for both structures, see also Table I, whereas our RA potentials with $p\text{H}_2$ and $o\text{H}_2$ are much more anisotropic. The well depths are ordered $\text{He} < \text{Ne} < p\text{H}_2 < o\text{H}_2 < \text{Ar}$, irrespective of the choice of the halogen molecule and for both minima. Equilibrium distances for the $p\text{H}_2\text{-X}_2$ and $o\text{H}_2\text{-X}_2$ complexes are similar to those of the respective He or Ne complexes.

Our findings are in line with the results by Darr *et al.* for the $\text{H}_2\text{-I}_2$ complex.³⁸ They experimentally identified a linear-shaped as the most stable and a T-shaped as the second most stable conformer. The experimental binding energy D_0 of the linear $o\text{H}_2\text{-I}_2$ complex is 1.42 kJ/mol and thus higher than the 1.22 kJ/mol found for $p\text{H}_2\text{-I}_2$. They also reported MP2/AVTZ well depths (D_e) for symmetric $\text{H}_2\text{-I}_2$ complexes and concluded that they lie between the values for the respective Ne and Ar complexes. Further, they analysed differences in the charge densities indicating a larger quadrupole-quadrupole interaction for the static *T2* structure compared to the *L* orientation.

In his thesis,³⁹ Tat Pham Van reported CCSD(T)/AV(DT)Z scans of the $\text{H}_2\text{-F}_2$ potential ΔE , fitted the results to a 5-site potential and calculated virial coefficients. Our calculations confirm the features of the $\text{H}_2\text{-F}_2$ potential and extend the angular and spatial resolution.

In addition, we have also collected effective RA pair potentials describing the interaction of $p\text{H}_2$ with other small molecules from the literature in the lower part of Table I. The one dimensional $p\text{H}_2\text{-pH}_2$ potential has a very low well depth of 0.296 kJ/mol and an equilibrium distance of 346 pm.^{44,75} The potential of $p\text{H}_2\text{-CO}$ has three minima.^{44,76} In contrast to $p\text{H}_2\text{-X}_2$, the global minimum corresponds to a slightly disturbed T-shaped complex with a well depth of 0.610 kJ/mol. Concerning the linear minima with well depths of 0.443 kJ/mol and 0.514 kJ/mol, $p\text{H}_2$ at the O side of CO is favoured.⁴⁴ Compared to the halogen interactions the potential is energetically less anisotropic. T-shaped global minimum structures were also found for the $p\text{H}_2\text{-OCS}$,^{15,77} $p\text{H}_2\text{-CO}_2$,^{44,78} $p\text{H}_2\text{-N}_2\text{O}$, and $o\text{H}_2\text{-N}_2\text{O}$ ⁷⁹ complexes. The anisotropy of these potentials, however is larger than found for the $p\text{H}_2\text{-X}_2$ potentials. An example for a triatomic molecule where a linear complex is stronger bound is HCN.^{80,81} In this complex, $p\text{H}_2$ binds stronger to the N-side and a distorted T-shaped structure is bound more weakly, although we have to note that this result is based on spherical averaging. For the $p\text{H}_2\text{-H}_2\text{O}$ complex, the rotational adiabaticization leaves only one minimum on the effective potential energy surface, where $p\text{H}_2$ is near a hydrogen nucleus of the water molecule.^{22,82} We conclude that $p\text{H}_2$ interacts less with CO than with F_2 . The strength of interaction with $p\text{H}_2$ is similar for F_2 , H_2O , and HCN. Concerning the values for D_e , $p\text{H}_2$

interacts stronger with CO₂ than with F₂ and even more with N₂O, OCS, Cl₂, and Br₂.

We have presented the fundamental RA pair potentials for the interaction of para- and ortho-hydrogen with fluorine, chlorine, and bromine, based on MP2 and CCSD(T) data. Hopefully, the present results will serve as a basis for further theoretical and experimental studies. From the RA potentials for $p\text{H}_2\text{-X}_2$ and $p\text{H}_2\text{-}p\text{H}_2$ ^{44,75} one can, in a pairwise fashion, approximate the many body potential of X₂($p\text{H}_2$)_{*n*} clusters with small *n*, where the H₂ rotational states are still mostly determined by the $p\text{H}_2\text{-X}_2$ interaction. However, when studying X₂($p\text{H}_2$)_{*n*} clusters with large *n*, the RA potentials for H₂-X₂ are of limited use, because the H₂ rotational dynamics may be dominated by the $p\text{H}_2\text{-}p\text{H}_2$ interaction. In such cases, it may be more convenient to use the tabulated 4D potentials provided in the supplementary material.⁶⁸

ACKNOWLEDGMENTS

The authors are grateful to Professor Dr. Jörn Manz for stimulating discussions and continuing support. The Computer Center (ZEDAT) of the Free University Berlin is acknowledged for using their computational resources. We thank the Deutsche Forschungsgemeinschaft (DFG) for the financial support provided through the collaborative research center (SFB 450).

- ¹M. S. Anderson and C. A. Swenson, *Phys. Rev. B* **10**, 5184 (1974).
- ²I. F. Silvera, *Rev. Mod. Phys.* **52**, 393 (1980).
- ³M. Rama Krishna and K. Whaley, *Z. Phys. D* **20**, 223 (1991).
- ⁴M. A. McMahon and K. B. Whaley, *Chem. Phys.* **182**, 119 (1994).
- ⁵F. Mezzacapo and M. Boninsegni, *Phys. Rev. Lett.* **97**, 045301 (2006).
- ⁶M. B. Sevryuk, J. P. Toennies, and D. M. Ceperley, *J. Chem. Phys.* **133**, 064505 (2010).
- ⁷S. Warnecke, M. B. Sevryuk, D. M. Ceperley, J. P. Toennies, R. Guardiola, and J. Navarro, *Eur. Phys. J. D* **56**, 353 (2010).
- ⁸A. Accardi, Ph.D. thesis, Department of Biology, Chemistry and Pharmacy, Freie Universität Berlin, 2012, available at http://www.diss.fu-berlin.de/diss/receive/FUDISS_thesis_000000040437.
- ⁹A. Einstein, *Ann. Phys.* **14**, 250 (2005).
- ¹⁰K. Rościszewski and B. Paulus, *Mol. Phys.* **108**, 2147 (2010).
- ¹¹O. Kühn, J. Manz, and A. Schild, *J. Phys.: Condens. Matter* **22**, 135401 (2010).
- ¹²K. Yoshioka, P. L. Raston, and D. T. Anderson, *Int. Rev. Phys. Chem.* **25**, 469 (2006).
- ¹³P. L. Raston and D. T. Anderson, *Low Temp. Phys.* **33**, 487 (2007).
- ¹⁴P. L. Raston, S. C. Kettwich, and D. T. Anderson, *Low Temp. Phys.* **36**, 392 (2010).
- ¹⁵F. Paesani, R. E. Zillich, and K. B. Whaley, *J. Chem. Phys.* **119**, 11682 (2003).
- ¹⁶F. Paesani, R. E. Zillich, Y. Kwon, and K. B. Whaley, *J. Chem. Phys.* **122**, 181106 (2005).
- ¹⁷F. Paesani and K. B. Whaley, *J. Chem. Phys.* **124**, 234310 (2006).
- ¹⁸H. Li, R. J. Le Roy, P.-N. Roy, and A. R. W. McKellar, *Phys. Rev. Lett.* **105**, 133401 (2010).
- ¹⁹P. L. Raston, W. Jäger, H. Li, R. J. Le Roy, and P.-N. Roy, *Phys. Rev. Lett.* **108**, 253402 (2012).
- ²⁰A. Michels, W. De Graff, and C. A. Ten Seldami, *Physica* **26**, 393 (1960).
- ²¹T. C. Lillestolen and R. J. Hinde, *J. Chem. Phys.* **136**, 204303 (2012).
- ²²P. Valiron, M. Wernli, A. Faure, L. Wiesenfeld, C. Rist, S. Kedžuch, and J. Noga, *J. Chem. Phys.* **129**, 134306 (2008).
- ²³J. Williams, A. Rohrbacher, D. Djahandideh, K. C. Janda, A. Jamka, F.-M. Tao, and N. Halberstadt, *Mol. Phys.* **91**, 573 (1997).
- ²⁴V. A. Apkarian and N. Schwentner, *Chem. Rev.* **99**, 1481 (1999).
- ²⁵K. W. Chan, T. D. Power, J. Jai-nhuknan, and S. M. Cybulski, *J. Chem. Phys.* **110**, 860 (1999).
- ²⁶R. Prosimiti, C. Cunha, P. Villarreal, and G. Delgado-Barrio, *J. Chem. Phys.* **116**, 9249 (2002).
- ²⁷M. Bargheer, A. Borowski, A. Cohen, M. Fushitani, R. B. Gerber, M. Gühr, P. Hamm, H. Ibrahim, T. Kiljunen, M. V. Korolkov *et al.*, *Analysis and Control of Ultrafast Photoinduced Reactions*, Springer Series in Chemical Physics Vol. 87 (Springer, Heidelberg, 2007), pp. 257–385.
- ²⁸A. Karpfen, P. Bunker, and P. Jensen, *Chem. Phys.* **149**, 299 (1991).
- ²⁹K. A. Peterson and T. H. Dunning, *J. Chem. Phys.* **102**, 2032 (1995).
- ³⁰Y. Qiu and Z. Bačić, *J. Chem. Phys.* **106**, 2158 (1997).
- ³¹J. S. Mancini and J. M. Bowman, "A new many-body potential energy surface for HCl clusters and its application to anharmonic spectroscopy and vibration-vibration energy transfer in the HCl trimer," *J. Phys. Chem. A* (published online).
- ³²J. Castillo-Chará, A. L. McIntosh, Z. Wang, R. R. Lucchese, and J. W. Bevan, *J. Chem. Phys.* **120**, 10426 (2004).
- ³³V. Aquilanti, S. Cavalli, F. Pirani, A. Volpi, and D. Cappelletti, *J. Phys. Chem. A* **105**, 2401 (2001).
- ³⁴W. B. Zeimen, J. Klos, G. C. Groenenboom, and A. van der Avoird, *J. Chem. Phys.* **118**, 7340 (2003).
- ³⁵G. Capecchi and H.-J. Werner, *Phys. Chem. Chem. Phys.* **6**, 4975 (2004).
- ³⁶J. Klos, M. M. Szczesniak, and G. Chalasinski, *Int. Rev. Phys. Chem.* **23**, 541 (2004).
- ³⁷J. E. Kenny, T. D. Russell, and D. H. Levy, *J. Chem. Phys.* **73**, 3607 (1980).
- ³⁸J. P. Darr, R. A. Loomis, S. E. Ray-Helmus, and A. B. McCoy, *J. Phys. Chem. A* **115**, 7368 (2011).
- ³⁹T. Pham Van, Ph.D. thesis, Universität zu Köln, 2006, available at <http://kups.uni-koeln.de/1897/>.
- ⁴⁰S. C. Kettwich, P. L. Raston, and D. T. Anderson, *J. Phys. Chem. A* **113**, 7621 (2009).
- ⁴¹M. V. Korolkov, J. Manz, and A. Schild, *J. Phys. Chem. A* **113**, 7630 (2009).
- ⁴²L. Pauling, *Phys. Rev.* **36**, 430 (1930).
- ⁴³A. F. Devonshire, *Proc. R. Soc. London, Ser. A* **153**, 601 (1936).
- ⁴⁴H. Li, P.-N. Roy, and R. J. Le Roy, *J. Chem. Phys.* **133**, 104305 (2010).
- ⁴⁵P. Jungwirth, P. Zdanska, and B. Schmidt, *J. Phys. Chem. A* **102**, 7241 (1998).
- ⁴⁶R. B. Gerber, M. V. Korolkov, J. Manz, M. Y. Niv, and B. Schmidt, *Chem. Phys. Lett.* **327**, 76 (2000).
- ⁴⁷T. Kiljunen, B. Schmidt, and N. Schwentner, *Phys. Rev. Lett.* **94**, 123003 (2005).
- ⁴⁸T. Kiljunen, B. Schmidt, and N. Schwentner, *Phys. Rev. A* **72**, 053415 (2005).
- ⁴⁹T. Kiljunen, B. Schmidt, and N. Schwentner, *J. Chem. Phys.* **124**, 164502 (2006).
- ⁵⁰A. Borowski and O. Kühn, *Theor. Chem. Acc.* **117**, 521 (2007).
- ⁵¹A. Borowski and O. Kühn, *Chem. Phys.* **347**, 523 (2008).
- ⁵²A. Accardi, A. Borowski, and O. Kühn, *J. Phys. Chem. A* **113**, 7491 (2009).
- ⁵³R. Ahlrichs, R. Penco, and G. Scoles, *Chem. Phys.* **19**, 119 (1977).
- ⁵⁴I. F. Silvera and V. V. Goldman, *J. Chem. Phys.* **69**, 4209 (1978).
- ⁵⁵D. S. Boucher, D. B. Strasfeld, R. A. Loomis, J. M. Herbert, S. E. Ray, and A. B. McCoy, *J. Chem. Phys.* **123**, 104312 (2005).
- ⁵⁶S. E. Ray, A. B. McCoy, J. J. Glennon, J. P. Darr, E. J. Fesser, J. R. Lancaster, and R. A. Loomis, *J. Chem. Phys.* **125**, 164314 (2006).
- ⁵⁷J. M. Pio, W. E. van der Veer, C. R. Bieler, and K. C. Janda, *J. Chem. Phys.* **128**, 134311 (2008).
- ⁵⁸J. Beswick, N. Halberstadt, and K. Janda, *Chem. Phys.* **399**, 4 (2012).
- ⁵⁹A. J. Stone, *The Theory of Intermolecular Forces* (Oxford University Press, 1997).
- ⁶⁰T. Helgaker, P. Jørgensen, and J. Olsen, *Molecular Electronic Structure Theory* (John Wiley and Sons, Inc., Chichester, 2000).
- ⁶¹B. Jeziorski, R. Moszynski, and K. Szalewicz, *Chem. Rev.* **94**, 1887 (1994).
- ⁶²H.-J. Werner, P. J. Knowles, G. Knizia, F. R. Manby, M. Schütz *et al.*, Molpro, version 2012.1, a package of *ab initio* programs, 2012, see <http://www.molpro.net>.
- ⁶³P. J. Knowles and N. C. Handy, *Chem. Phys. Lett.* **111**, 315 (1984).
- ⁶⁴H.-J. Werner and P. J. Knowles, *J. Chem. Phys.* **89**, 5803 (1988).
- ⁶⁵T. H. Dunning, *J. Chem. Phys.* **90**, 1007 (1989).
- ⁶⁶K. A. Peterson, D. Figgen, E. Goll, H. Stoll, and M. Dolg, *J. Chem. Phys.* **119**, 11113 (2003).
- ⁶⁷S. F. Boys and F. Bernardi, *Mol. Phys.* **19**, 553 (1970).
- ⁶⁸See supplementary material at <http://dx.doi.org/10.1063/1.4892599> for data points and fit coefficients.

- ⁶⁹A. Bondi, *J. Chem. Phys.* **68**, 441 (1964).
- ⁷⁰J. R. Krumrine, S. Jang, M. H. Alexander, and G. A. Voth, *J. Chem. Phys.* **113**, 9079 (2000).
- ⁷¹D. T. Moore, M. Ishiguro, and R. E. Miller, *J. Chem. Phys.* **115**, 5144 (2001).
- ⁷²S. Moroni, M. Botti, S. D. Paolo, and A. R. W. McKellar, *J. Chem. Phys.* **122**, 094314 (2005).
- ⁷³H. Zhu and D. Xie, *J. Comput. Chem.* **30**, 841 (2009).
- ⁷⁴F. Paesani and K. B. Whaley, *Mol. Phys.* **104**, 61 (2006).
- ⁷⁵K. Patkowski, W. Cencek, P. Jankowski, K. Szalewicz, J. B. Mehl, G. Garberoglio, and A. H. Harvey, *J. Chem. Phys.* **129**, 094304 (2008).
- ⁷⁶P. Jankowski and K. Szalewicz, *J. Chem. Phys.* **123**, 104301 (2005).
- ⁷⁷K. J. Higgins, Z. Yu, and W. Klemperer, in *Proceedings of the 57th Ohio State University International Symposium on Molecular Spectroscopy, Columbus, OH, 17–21 June 2002*, Paper RA02 (unpublished).
- ⁷⁸H. Li, P.-N. Roy, and R. J. Le Roy, *J. Chem. Phys.* **132**, 214309 (2010).
- ⁷⁹L. Wang, D. Xie, R. J. Le Roy, and P.-N. Roy, *J. Chem. Phys.* **139**, 034312 (2013).
- ⁸⁰D. B. Abdallah, F. Najjar, N. Jaidane, F. Dumouchel, and F. Lique, *Mon. Not. R. Astron. Soc.* **419**, 2441 (2012).
- ⁸¹O. Denis-Alpizar, Y. Kalugina, T. Stoecklin, M. H. Vera, and F. Lique, *J. Chem. Phys.* **139**, 224301 (2013).
- ⁸²T. Zeng, H. Li, R. J. Le Roy, and P.-N. Roy, *J. Chem. Phys.* **135**, 094304 (2011).